In-vitro and in-silico investigation of α-amylase and α-glucosidase inhibition using Chamaecostus cuspidatus leaf for diabetes mellitus

Menaka Priya Balaji
Vellore Institute of Technology University
V Devi Rajeswari
vdevirajeswari@vit.ac.in

Vellore Institute of Technology University

Research Article

Keywords: Antidiabetic, Anti-inflammatory, HepG2, Chamaecostus cuspidatus, Docking

Posted Date: March 1st, 2024

DOI: https://doi.org/10.21203/rs.3.rs-3990166/v1

Additional Declarations: No competing interests reported.

Abstract

Chamaecostus cuspidatus is a mysterious plant with potential therapeutic properties for the amelioration of diabetic mellitus and related complications. This investigation aims to determine the potential phytochemicals through GCMS, FTIR, and NMR techniques. The objective is to perform in-vitro assays on the extract to evaluate its potential in various domains including antioxidant, antidiabetic, anti-inflammatory, antibacterial, and anticancer effects. The extract of methanol has demonstrated significant antioxidant properties due to its high phenolic content (3.523 mg GAE/g), flavonoid content (2.55 mg QE/g), and total tannin content (2.133 mg TAE/g). GC-MS analysis of leaf extract depicted the presence of 16 bioactive compounds among 9-octadecenamide, 7-nonenamide, 13-docosenamide, and hexadecanamide are enrich essential fatty acids. The NMR spectrum of ^{13}C confirms the presence of functional bioactive compounds. This work includes molecular computational studies, specifically protein-ligand docking energy and ADMET analysis. Selected screened compounds including akuammilan-17-ol, nor-diazepam, 1,2-benzene dicarboxylic acid, and standard metformin were investigating the interaction against α-amylase and α-glucosidase. The ligand of nor-diazepam showed the highest binding affinity compared to akuammilan-17-ol, 1,2-benzene dicarboxylic acid, and metformin; therefore, nor-diazepam could be the focus of more in-depth research.

Introduction

Diabetes mellitus is one of the largest epidemic emergencies of this modern era, by the year 2035 predicted diabetes is 592 million all around the world [1]. Diabetes mellitus is a multifactorial condition that can be caused by various factors including a sedentary lifestyle, a diet high in sugar [2], genetic predisposition resulting in inadequate production of insulin, and autoimmunity or defective insulin action in cells. The biological process of continuous glucose absorption mediated by the catalysis and breakdown of α-amylase and α-glucosidase enzymes is probably the most significant contributor that triggers hyperglycemia. Since it is widely recognized, α-amylase breaks down the glycosidic bonds in starch to produce disaccharides, which are subsequently further broken down by mucosal α-glucosidase in enterocytes. This process accelerates glucose absorption and elevates blood glucose levels post-diet. Persistent hyperglycemia causes cellular stress and the generation of advanced glycation end product which in turn dysregulate cellular metabolism and gradually release pro-inflammatory cytokines [3]. Therefore, minimizing the bloodstream and gastrointestinal absorption of glucose is a beneficial and efficient technique for treating hyperglycemia. This can only be managed by suppressing the digestive enzymes including α-amylase and α-glucosidase [4] [5]. Currently, antidiabetic oral enzyme inhibitors approved by the Food and Drug Administration (FDA) may have adverse effects, and people eventually prefer herbal medicine which becoming an attractive treatment for new diseases [6].

Traditional herbal medicines have been theorized to possess drug-like properties in certain metabolites, which are believed to have a substantial impact on promoting overall well-being and preventing multiple illnesses while avoiding any adverse effects. This study primarily focuses on intermediate secondary metabolites that possess drug-like structures [7]. This approach may lead to the identification of novel,

unstudied compounds with the potential for treating complex diseases by exploring unexplored herbs. This study specifically focused on the species of monocot in the family Costaceae, commonly known as the insulin plant (Taxonomy ID: 168191). The study aimed to analyze the phytochemical composition of *C. cuspidatus* using different polarity solvent maceration extraction and identify the potential extract by preliminary studies and compound characterization. Additionally, we investigate the antidiabetic, antioxidant, anti-inflammatory, antibacterial, and anticancer potential to find IC_{50} value. Further, GCMS-identified potential compounds were screened by druglikeness rule and absorption, distribution, metabolism, excretion, and toxicity properties for molecular docking study prediction. Following the evaluation of selected compounds, a docking study was carried out on a certain number of ligands to observe the interaction and affinity with the α-amylase and α-glucosidase proteins. The outcome could bring light to a method for the deliberate identification of novel compounds and enable new perspectives on the application of herbal plants in the treatment of diabetes mellitus.

Materials and methods

Chemicals

Porcine pancreatic α-amylase (10 units/mg), starch, (DPPH) 2,2'-diphenyl-1-picrylhydrayl, sodium carbonate, p-Nitrophenyl-α-D-glucopyranoside, ascorbic acid, 3-[4,5-dimethylthiazol-2-yl]-2,5 diphenyl tetrazolium bromide, and bovine serum albumin (BSA), were all purchased from HiMedia chemicals, India. HPLC grade acetonitrile and methanol, gallic acid, quercetin, tannic acid, α-glucosidase (1U/mL), trichloroacetic acid, metformin hydrochloride, diclofenac sodium, ABTS (2,2’-Azino-bis (3-ethylbenzothiazoline-6-sulfonic acid) diammonium salt, metformin, penicillin-streptomycin and Dulbecco’s Modified Eagle Medium (DMEM) from Sigma-Aldrich.

Collection and identification of the plant

C. cuspidatus was collected in November month from Yelagiri mountain in the Tirupathur district of Tamil Nadu, India. The plant sample was taxonomically identified by Prof. P. Jayaraman, Director of Plant Anatomy Research Centre (PARC), West Tambaram, Chennai. The identification was conducted under the authorization number PARC/2022/4736.

Preparation of extract

The leaf of *C. cuspidatus* was separated into parts and all possible impurities were meticulously removed using deionized water. The cleaned leaf parts were then dried in a shaded area at a temperature of 38^{o}C. In a processor, the chopped leaf components were then ground into a powder. The fine leaf powder was stored in a dry and sealed container, protected from sunlight and moisture. To the maceration, course-dried leaf powder was mixed with different polarity solvents (distilled water, methanol, chloroform, ethyl acetate, hexane). Following that, the extract performed filtration using a muslin cloth. The extracts were concentrated through a rotary evaporator and refrigerated for further application [8].

Qualitative Evaluation of C. cuspidatus Leaf

The extraction required primary phytochemical analysis to determine the major bioactive components contained in the different polarity solvent extract [9]. Standard chemical procedures were employed for evaluating a plant extract [10].

Fourier Transform Infrared Spectroscopy

The concentrated extracts were subjected to analysis using FTIR (IR-affinity-1, SHIMAZDU, Japan 2011) to identify predominant functional groups and stretching and bending vibrations in different solvent samples within the range of 400–4000 cm^{-1}. Further, screen the effective extract based on the preliminary and IR spectrum.

Gas Chromatography-Mass Spectrometry Analysis

The selected methanolic leaf extract of *C. cuspidatus* was analyzed using GC-MS on the Perkin Elmer Clarus 600 C model from the USA. Phytochemical identification was achieved by determining a retention time of 30 minutes and comparing the MS of the identified substance.

Nuclear Magnetic Resonance Spectroscopy

The methanolic extract of *C. cuspidatus* was dissolved (20 mg/mL) in deuterated DMSO and subjected to sonicated for 15 minutes and centrifuge at 2500 rpm for 5 minutes. 800 µL of supernatant was transferred to the NMR tube [11]. The sample was analyzed using NMR Spectroscopy specifically FT-NMR at a frequency of 400 MHz using a Bruker instrument.

Determination of Total Phenolic Content

The Folin-Ciocalteu method was used to determine the total phenolic content, as explained by Ramasubramaniyan et al. (2015) with minor changes. A gallic acid curve was calculated by diluting a standard gallic acid (1 mg/mL stock) solution to varying concentrations (5, 25, 50, 75, and 100 µL) in methanol [13]. 2.5 mL of Folin-Ciocalteu reagent was mixed with the unknown sample, and the mixture was incubated for 5 to 8 minutes at 38^{o}C. Two milliliters of a 75% sodium carbonate solution were added and the mixture was incubated at a temperature of 50^{o}C for a duration of 10 to 15 minutes. At OD_{765} nm, the reaction mixture's absorbance was measured. Using a calibration curve based on gallic acid and reported in milligrams of gallic acid equivalent per gram (mg GAE/g), the phenolic content of the unknown sample was determined.

Determination of Total Flavonoid Content

The total flavonoid content was estimated using an aluminum chloride colorimetric assay, following the method described by Nikzad and Parastar (2021) with slight modifications. 1 mg/mL of quercetin standard with various concentrations (5, 25, 50, 75, and 100 µL) and 1 mL unknown sample. The resulting mixture was mixed with 200 µL of 10% aluminum chloride. 1 M of 200 µL potassium acetate was mixed and 5.6 mL of milli-Q water was incubated for 3 to 5 mins [15]. UV spectrophotometer was

used to evaluate the absorbance of the standard and sample solution at 415 nm in comparison to the reagent blank. The flavonoid content of the unknown sample was quantified using a quercetin calibration curve, reported in milligrams of quercetin equivalent per gram (mg QE/g).

Determination of Total Tannin Content

The Folin-Ciocalteu method was used to calculate the total tannin concentration [16]. A tannin acid standard with a concentration of 1 mg/mL of tannic acid standard with various concentrations (5, 25, 50, 75, and 100 µL) and 0.5 ml of Folin-Ciocalteu reagent in a final volume of 10 mL milli-Q water was mixed in the reaction. The reaction mixture was incubated for 30 mins and the absorbance was measured at 700 nm. Using a tannic acid equivalent curve, the tannin content of the unknown sample was determined and reported in milligrams of tannin acid equivalent per gram (mg TAE/g).

Evaluation of Antioxidants by Invitro Techniques

Activated oxygen species which include single molecule oxygen and (H_2O_2) hydrogen peroxide, can cause cell damage by reacting with free radicals [17] [18]. We performed the FRAP, ABTS, and DPPH assays to assess the reducing potency and radical scavenging properties. Various aliquots (5, 25, 50, 75, and 100 mg/mL) of the sample, along with ascorbic acid as a positive control. A blank for antioxidant activities was created using a phosphate buffer and methanol. To assess the reduction of Fe^{3+} to Fe^{2+}, we conducted the FRAP assay. A mixture of 1 mL methanol solution (sample and standard) and phosphate buffer (pH 6.6) was prepared. Subsequently, the reaction mixture was treated with 1% of 2.5 mL potassium ferricyanide solution [19]. The reactant was vigorously and subjected to incubation at a temperature of 50^oC for a duration of 20 to 30 minutes. Following this, 10% of 2.5 mL trichloroacetic acid was added and the solution was centrifuged at 3000 rpm for 3 minutes. The supernatant was diluted with an equal volume of mill-Q water. Then, 0.5 mL of ferric chloride (20 mM) was added and incubated for 2 to 3 minutes. Using a UV spectrophotometer, the absorbance of the reaction mixture was determined at 700 nm. The 2 mL of extract was mixed with a DPPH (0.1 mM) and incubated in darkness for a duration of 30 minutes. The absorbance of the reaction was measured at wavelength of 517 nm. The ABTS activity was determined by mixing a reaction mixture of 7 mM ABTS solution with 2.45 mM potassium persulfate to generate radical cations. 1 mL volume of both sample and standard solution were mixed with 2 mL of ABTS radical cation reactant solution. The resulting mixture was then incubated for duration of 25 to 30 minutes. The reaction was quantified at wavelength of 734 nm [20]. The inhibition potential percentage was determined through the employing of an equation.

$$\%Inhibition = \frac{Acontrol - Asample}{Acontrol} * 100$$

Evaluation of Antidiabetic by In-vitro Techniques

The evaluation of α-amylase and α-glucosidase enzyme inhibition has gained considerable interest in the analysis of blood hemostasis. Subsequently, the α-amylase and α-glucosidase enzyme inhibition of the samples (10 to 100 mg/mL) was evaluated using 0.1 mL of each sample [21]. Metformin was employed

as a positive correlation with the samples [22] [23]. The α-amylase inhibitory assay was assessed using the standard DNS method. Difference sample and standard concentration solutions were treated with 0.2 M of 500 µL phosphate buffer (pH 6.9) and 1 U/mL amylase enzyme solution. The reaction was incubated for 20 to 30 minutes at 38^{o}C. A 250 µL aliquot of 1% starch solution was incubated for 15 minutes. To terminate the reaction, 1 mL of DNS reagent was added and incubated in a boiling water bath for 10 to 15 minutes. The results were measured at a wavelength of 540 nm. The α-glucosidase inhibitory assay was assessed using the para nitrophenyl α-D-glucopyranoside substrate method. The experiment involved using 0.1 M 150 µL phosphate buffer (pH 6.9) as the sample and standard concentrations. Additionally, 1 U/mL of glucosidase enzyme was added to initiate the enzyme reaction. The reaction was incubated for 10 to 12 minutes. The enzyme reaction was terminated by adding 50 µL of 2mM PNP substrate and incubating the reaction mixture for a duration of 15 to 20 minutes. The enzyme reaction was terminated using 50 µL of 0.1 M sodium carbonate, and the resulting measurement was taken at 405 nm.

$$\%Inhibition = \frac{Acontrol - Asample}{Acontrol} * 100$$

Invitro Bovine Serum Albumin Assay

Bovine serum albumin (BSA), when subjected to heat, undergoes denaturation and initiates the expression of the antigen-associated response. The anti-denaturation assay is evaluated as a significant method for stabilizing compounds against allergies [24]. Various concentrations of (2.5, 5, 25, 50, 75, and 100 mg/mL) were evaluated and compared to a positive control to diclofenac [25]. A 0.2% solution of BSA was prepared using phosphate buffer at pH 6.5. A 1 mL sample and standard were subjected to treatment with 500 µL of BSA solution. The resulting reaction mixture was heated at 60^{o}C for a duration of 2 to 4 minutes. After cooling, the reaction was incubated for a period of 15 to 20 minutes [26]. The UV-visible spectrophotometer was used to measure the absorbance of the solution at a wavelength of 520 nm [27].

$$\%Inhibition = \frac{Acontrol - Asample}{Acontrol} * 100$$

Antibacterial activity

The antibacterial activity of three different bacterial strains including *Escherichia coli, Klebsiella pneumonia*, and *Staphylococcus aureus*, was examined against the methanolic leaf extract of *C. cuspidatus* methanolic leaf extract. Muller Hinton Agar served as the substrate for the agar diffusion procedure, and plates were then utilized using the standardized microbe culture method performed in Muller Hinton Agar (MHA), plates were lawn cultured with standardized microbial culture broth. Plant extract showed indeed effectiveness so, the concentration of the sample was fixed with a microgram. 20 µL of the plant extract was poured into each well after it had been dissolved in 1% DMSO using distilled

water. The plates were incubated at 37^{o}C for an extended period. Following incubation, the emergence of a clear zone around the well proved. The size of the zone of inhibition was measured and evaluated. For positive control, an ampicillin antibiotic disc was utilized.

Cell culture - MTT assay

The absorption phase of a drug is crucial for its effectiveness, as it determines the degree to which the drug is taken up by liver cells. Therefore, it is important to perform cytotoxic analysis to assess the effect of the drug on the HepG2 cell line. The HepG2 cell line, provided by the National Centre for Cell Science, Pune (NCCS), was utilized to evaluate the cytotoxicity of a leaf sample from *C. cuspidatus.* The cells were maintained in Dulbecco's Modified Eagle Medium (DMEM media) supplemented with 10% fetal calf serum and penicillin (100 U/mL) in a humidified environment. The cells were cultured at 37^{o}C in a temperature-controlled atmosphere containing 5% CO_2 and 95% atmosphere [28]. The MTT (3-[4,5-dimethylthiazol-2-yl]-2,5 diphenyl tetrazolium bromide) test was conducted using varying concentrations of the sample to determine cell viability [25]. The absorbance at 540 nm was calculated using a UV spectrophotometer [29].

$$\%ofCellviability = HepG2of\frac{Treatedcells}{Controlcells} * 100$$

In silico study

Druglikeness rule and ADMET analysis

The importance of pharmacokinetic and pharmacodynamic studies in determining standard drug design through the process of drug-likeness is expanding. Limited studies have examined the screening of compound parameters in the overall framework of target drug design. All compounds were evaluated and screened using Lipinski's rule of five [30], Pfizer rule, GSK, and the golden triangle, and further selected screened compounds investigated the ADMET properties for molecular docking. To objective is to assess the pharmacokinetics and toxicity of *C. cuspidatus* screened lead compounds utilization of the SwissADME (www.swissadme.ch) online tool. In addition to its conformation, ADMETlab 2.0 used canonical smiles to forecast ligand characteristics and determine their pharmacokinetics, potentially lowering the hazards involved in upcoming research studies.

Molecular docking

The crystal structure of α-amylase (1B2Y) and α-glucosidase (5NN8) was retrieved from the RCSB protein data bank with the co-crystallized inhibitor of acarbose. Molecular docking analysis is employed to forecast the binding between ligands and proteins in biological activities, facilitating recognition of molecular biology and computer-aided design. According to the literature survey, 1B2Y protein (X = 18.909389; Y = 5.79070; Z = 47.006148) and 5NN8 protein (X = 12.10300, Y= -16.549000, Z = 106.548000) exhibit the active sites which allowing the ligand to identification of high-affinity binding compounds. Various software tools, including Autodock, Autodock vina package v1.2.3, MGL software, and Discovery

Studio are utilized for virtual molecular docking. Protein Data Bank was used to obtain 3D crystallographic structures of proteins (www.rcsb.org). the protein complex was selected for analysis after removing water molecules, heteroatoms, and inhibitors. Subsequently, the PDBQT format was generated [31].

The screened ligands of nor-diazepam, akuammilan-17-ol, 1,2-benzene dicarboxylic acid, and standard metformin were used in the molecular docking study, ligands were obtained from the PubChem database (pubchem.ncbi.nlm.nih.gov) and prepared for analysis in PDBQT format using CADD group Chemoinformatics tools (cactus.nci.nih.gov) and Autodock vina software. Proteins and ligands possessed a total of 10 degrees of freedom. Among the 10 binding poses generated, the initial negative binding pose had a lower root mean square deviation (RMSD) value of atomic alignment. This result suggests that the initial negative binding pose is highly valid and indicates a stronger binding efficacy. The binding affinity was determined, and the ligand's predicted pose was analyzed. The interactions of the 2D results were visualized using Discovery Studio.

Statistical Analysis

The experiments were conducted in triplicate, and the quantitative analysis data were subjected to regression analysis in Microsoft Excel. The in vitro results were analyzed using OriginPro software while the IC_{50} value was determined in Microsoft Excel. The in vitro anticancer activity results were analyzed using GraphPad Prism 8 and Dunnett's test. A significance level of $P < 0.005$ was employed.

Results

Extraction Yield

By utilizing the maceration method, the highest yield was obtained from a methanol extract of 10.65% followed by Aqueous > Chloroform > Hexane > Ethyl acetate. The total yield of different solvent values is given in Table 1.

Table 1
Yield of different solvents of *Chamaecostus cuspidatus* leaf

Extraction	Color	Extract Yield (%)
Aqueous extract	Solid dark brown	9.03
Methanol extract	Semi-solid dark brown	10.65
Ethyl acetate	Semi-solid dark blackish-green	7.42
Chloroform	Solid dark green	8.17
Hexane	Semi-solid dark greenish brown	8.07

Qualitative and Quantitative Evaluation of C. cuspidatus leaf

Plant secondary metabolites play a significant role in herbal medicine and possess various potential applications. The analysis revealed the presence of flavonoids, phenols, and cardiac glycosides are more abundant in the methanolic extract. Following methanol extract, aqueous extract shows good results. Among all phytochemical tests, chloroform and hexane reveal the presence of steroid and saponin chemicals. Among all extracts chloroform, and hexane showed less than ethyl acetate extract. A preliminary analysis of *Chamaecostus cuspidatus* leaf in different solvent evaluations is given in Table 2.

Table 2
Identification of phytochemical screening of *Chamaecostus cuspidatus* leaf extraction.

Phytochemical	Aqueous	Methanol	Ethyl acetate	Chloroform	Hexane
Alkaloids	+	+	-	-	-
Protein	+	+	-	-	-
Carbohydrate	+	+	+	+	+
Reducing sugar	+	+	-	-	-
Cardiac glycoside	+	++	-	-	-
Flavonoids	+	+	+	-	-
Terpenoids	+	+	-	-	-
Phenols	+	++	-	-	-
Saponin	+	+	+	+	+
Steroid	-	-		++	+
Tannin	+	+	-	-	-

Note: ++ indicated that immediate positive reaction, + indicated the presence of phytochemicals, - indicated that the absence of the reaction

Fourier Transform Infrared Spectroscopy

FTIR spectroscopy was utilized to analyze the bioactive compounds present in the leaves of the *C. cuspidatus* leaf. The FTIR spectra were used to separate the functional and active components of the different polarity extracts by analyzing their spectrum. Table 3 and graph represented in Fig. 1, IR frequency indicating the presence of ester and anhydride functional group in chloroform and ethyl acetate extraction whereas methanol shows phenol and amide group. Aqueous extract reveals the presence of acid and halide groups. When compared to other extract frequencies hexane showed the least function bioactive compounds.

Table 3
FTIR analysis of *Chamaecostus cuspidatus* leaf extract

Frequency range (cm^{-1})	Compound class	Absorption range (cm^{-1})	Functional group
500–800	Alkyl halides	512	C-I
		604	C-Br
		714	C-Cl
1060–1100	Phenol/alcohol	1076	C-O
1020–1250	Amine/ester	1044	C-N
		1239	C-O
		1168	C-N
1760–1900	Acid/anhydride	1890	C = O
900–1300	Anhydride	1371	C-O
1450–1465	Alkane	1468	C-H
1638–1648	Alkene	1644	C = C
1710–1740	Ketone/aldehydes/ester	1739	C = O
2840–3000	Alkane	2924	C-H
3000–3100	Aromatics	3347	C-H

Gas Chromatography-Mass Spectrometry Analysis

Phytocompounds were identified using Gas chromatography and Mass spectroscopy. The chromatogram of the methanolic extract can be seen in Fig. 2. The chromatogram displayed 10 distinct peaks, confirming the retention time range between 3 and 30 minutes. The National Institute of Standards and Technology (NIST) library database provided a preliminary identification of phytochemical constituents. Table 4 presents the results of mass spectrometry analysis, which confirmed the presence of intermediate compounds and secondary metabolites. Among 16 compounds from the methanol extract of *C. cuspidatus* leaf showing major peak of 23.52 corresponds to the presence of four amide-fatty acids in the Costaceae family including 9-octadecenamide, 7-nonenamide, 13-docosenamide, and hexa-decanamide. The peaks observed at 18.00 and 21.52 correspond to the presence of (an indole derivative compound) akuammilan-17-oL, the 19.43 peak corresponds to the presence of nor-diazepam, and the 15.65 peak corresponds to the presence of 1,2-benzene dicarboxylic acid. These compounds were identified based on retention time, molecular formula, structure, and molecular mass (M.M).

Table 4
GC-MS data of *Chamaecostus cuspidatus* leaf

S. No	Name of the Compound	Molecular Mass (g/mol)	Molecular formula	Retention Time
1	9-Octadecenamide	281.5	$C_{18}H_{35}NO$	23.54
2	7-Nonenamide	155.24	$C_9H_{17}NO$	23.54
3	13-Docosenamide	337.6	$C_{22}H_{43}NO$	23.54
4	Hexadecanamide	255.44	$C_{16}H_{33}NO$	23.54
5	Pentadecanamide	319	$C_{15}H_{30}ONBr$	23.54
6	8,11,14-Eicosatrienoic acid	306.5	$C_{20}H_{34}O_2$	21.91
7	Akuammilan-17-ol	324.4	$C_{20}H_{24}N_2O_2$	21.52
8	Octadecanoic acid	284.5	$C_{18}H_{36}O_2$	19.78
9	Eicosanoic acid	312.5	$C_{20}H_{40}O_2$	19.78
10	Docosanoic acid	340.6	$C_{22}H_{44}O_2$	19.78
11	Nor-diazepam	373.8	$C_{18}H_{16}ClN_3O_4$	19.39
12	8-Quinolinedione	452.1	$C_{17}H_{12}Br_2N_2O_3$	18.00
13	Phthalic acid	330.4	$C_{20}H_{26}O_4$	15.65
14	1,2-Benzene dicarboxylic acid	222.24	$C_{12}H_{14}O_4$	15.65
15	1,3-diethyl 2-cyclohexylpropanedioate	242.31	$C_{13}H_{22}O_4$	8.03
16	2,4,6,8,10-Tetradecapentaenoic acid	606.7	$C_{36}H_{46}O_8$	6.79

Nuclear Magnetic Resonance Spectroscopy

NMR spectroscopy was used to analyze the methanolic extract of the *C. cuspidatus* plant according to the ^{13}C nuclei. The quantitative analysis, despite its non-sensitive nature, provided information about a limited number of chemical structures, including the DMSO peak. The NMR spectrum of ^{13}C nuclei detected the presence of carbon atoms in the sample, a result represented in Fig. 3. Specifically, the sample contained a total of 16 carbon atoms, a peak at 39.20–40.45 ppm indicating the presence of the solvent. A peak at 20.49–29.45 ppm indicates the presence of CH; 61.61–102.42 ppm indicates the presence of C ≡ C; 128.39 ppm indicates the presence of an aromatic ring in the aromatic ring; 162.60 ppm indicates the presence of OH group.

Quantitative analysis

The Folin-Ciocalteu reagent was used to calculate the total phenolic content of the plant extract (Fig. 4), while the total flavonoid content was assessed as aluminum chloride (Fig. 5). The total tannin content was analyzed using the Folin-Ciocalteu method (Fig. 6). The *C. cuspidatus* plant sample exhibited 3.523 mg GAE/g, followed by 2.550 mg QE/g for flavonoids, and 2.133 mg TAE/g for tannins.

Invitro Antioxidant Activities

The antioxidant assays of the *C. cuspidatus* were determined by FRAP, ABTS, and DPPH assays. The scavenging effect of plant samples was compared with positive control of ascorbic acid. The FRAP assay demonstrated the conversion of ferric 2,4,6 tripyridyl-5-triazine (Fe^{3+}) to ferrous (Fe^{2+}), indicating the presence of phenolic compounds with strong antioxidant activity. This experiment demonstrated a dose-dependent scavenging effect of 700 nm. For FRAP, a concentration of 100 mg/mL showed an inhibition percentage of 55.85%, and the IC_{50} value was determined to be 82.2 mg/mL (Fig. 7). When compared to the plant sample, the standard of ascorbic acid showed a significant scavenging effect on the DPPH radical. This effect increased with higher concentrations of 2.5, 5, 25, 50, 75, and 100 mg/mL. For FRAP, the plant sample at a maximum concentration of 100 mg/mL showed 62.51% inhibition with an IC_{50} value of 76.25 mg/mL (Fig. 8). When compared to the positive control of ascorbic acid, the scavenging effect of the plant sample was similar. The ABTS radical scavenging activity of the plant extract indicated a high presence of phenol compounds, which effectively inhibited the ABTS radicals (2,2'-Azino-bis (3-ethylbenzothiazoline-6-sulfonic acid). The maximum concentration of 100 mg/mL resulted in 79.14% inhibition, while ascorbic acid exhibited 96% inhibition and the IC_{50} value of the plant sample was determined to be 51.05 mg/mL (Fig. 9).

Invitro Antidiabetic activities

Antidiabetic activities of methanolic extract of *C. cuspidatus* leaf extract exhibited α-amylase inhibition, indicating the potential of compounds that are inhibitory against the enzyme. The plant sample exhibited a significant inhibitory effect of 69% on the α-amylase enzyme, while the control metformin demonstrated a higher inhibition range of 73.12% at a concentration of 100 mg/mL. The IC_{50} value of α-amylase inhibition of the plant sample was determined to be 78.2 mg/mL 0.953 (Fig. 10). Following, the sample exhibited an α-glucosidase inhibitory activity of 59.12% at a concentration of 100 mg/mL, whereas the control metformin demonstrated an inhibition activity of 82.65% (Fig. 11). The IC_{50} value of the plant sample was found at 82.64 mg/mL.

Invitro Anti-inflammatory activity

Inhibition of protein denaturation was determined by bovine serum albumin and the sample effectively inhibited heat-induced albumin protein. At a maximum concentration of 100 mg/mL exhibited a 58% inhibition, while the positive control of diclofenac sodium standard showed 88% inhibition. The IC_{50} value of the plant sample was determined to be 44.65 mg/mL. The plant sample exhibited significantly reduced

inflammation, indicating potential non-steroidal anti-inflammatory properties in the *C. cuspidatus* leaf sample. The positive correlation experiment of the protein degradation assay was reported in Fig. 12.

Antibacterial activity

To control gastrointestinal probiotics, it is important to examine the antibacterial potential to maintain the gut microbiome. By measuring the zone of inhibition (mm), the three bacterial strains' agar well diffusion against methanolic extract was observed. It was noted that *S. aureus* showed more potential inhibition than *E. coli* and *K. pneumonia* in terms of effectiveness. Tables 5 and 6 illustrate the findings of the highest efficient bacterial inhibition at a concentration of 100 µg among the varied concentrations.

Table 5
Antibacterial measurement of the zone of inhibition

Bacterial strain	5 µg concentration (mm)	25 µg concentration (mm)	50 µg concentration (mm)	100 µg concentration (mm)
Escherichia coli	-	-	-	2
Klebsiella pneumonia	-	-	-	10
Staphylococcus aureus	-	10	14	16

Table 6. Antibacterial activity of *Chamaecostus cuspidatus* leaf extract against bacteria.

Escherichia coli	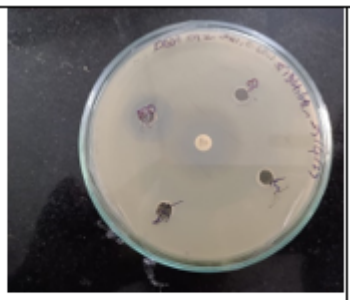	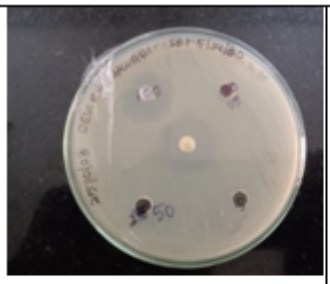	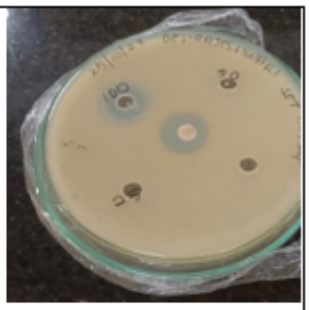
Klebsiella pneumonia		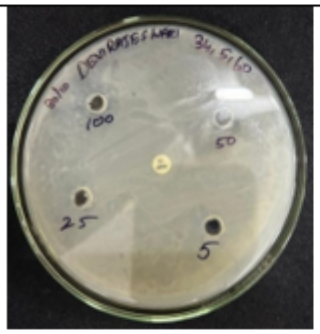	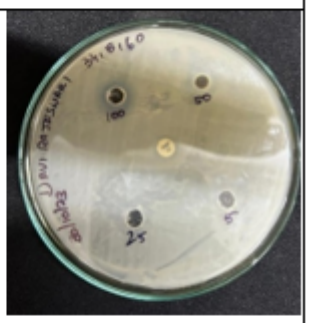
Staphylococcus aureus	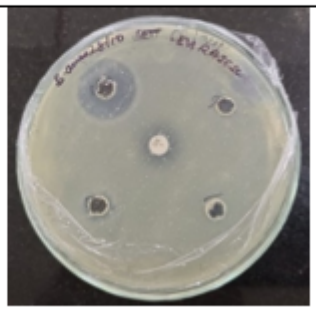	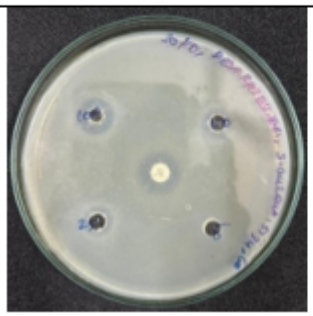	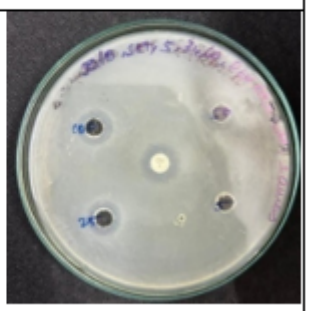

Anticancer activity

This cytotoxicity assay is employed to assess cell viability and determine the toxic dose for cancer cells. Similarly, *C. cuspidatus* demonstrated toxicity to HepG2 cells based on dosage. The crude extract was analyzed and it was found that MMS exhibited notable cytotoxicity towards the hepatic (HepG2) cell line, as demonstrated using the MTT assay. The concentrations selected for assessment yielded an IC_{50} value of 165.21 mg/mL (Fig. 13). These findings demonstrate that the plant extract from *C. cuspidatus* effectively inhibited the growth of cancer cells in a dose-dependent manner, with a significant level of inhibition.

Computational studies

Screening of lead molecule

Based on the GCMS result 16 compounds have been demonstrated in drug-likeness analysis using ADMETlab 2.0 and the Swiss ADME online tool which is significant for prediction of biological activity and further studies (Supplementary file). Among all compounds, three ligands fulfilled drug-likeness rules including nordiazepam, 1,2-benzene dicarboxylic acid, and akuammilan-17-oL. These three ligands were

selected for drug-likeness evaluation and pharmacokinetics property investigation with standard metformin (Table 7).

Table 7
Drug-likeliness rule and ADMET property of metformin, akuammilan-17-ol 1,2-benzene dicarboxylic acid, and nor-diazepam.

Drug-likeliness rule and ADMET Property	Metformin	Akuammilan-17-ol	1,2-Benzene dicarboxylic acid	Nor-diazepam
Molecular weight (g/mol)	129.16	324.42	222.24	373.79
Rotatable bond	2	2	6	5
H bond acceptor	2	4	4	5
H bond donor	3	1	0	2
Consensus Log P	-0.89	2.43	2.30	2.06
Molar refractivity	36.93	102.24	58.61	103.20
Topological polar surface area ($Å^2$)	91.49	45.06	52.60	91.23
Lipinski	Yes	Yes	Yes	Yes
Ghose	No	Yes	Yes	Yes
Veber	Yes	Yes	Yes	Yes
Egan	Yes	Yes	Yes	Yes
Bioavailability score	0.55	0.55	0.55	0.55
CYP1A2 inhibitor	No	No	Yes	No
CYP2C19 inhibitor	No	No	No	No
CYP2D9 inhibitor	No	No	No	No
CYP2D6 inhibitor	No	No	No	No
CYP3A4 inhibitor	No	Yes	No	Yes
Clearance	3.531	11.97	12.247	3.514
hERG Blocker (KCNH2)	0.176	0.025	0.136	0.225
Drug-induced liver injury	0.101	0.119	0.404	0.985
AMES toxicity	0.024	0.093	0.013	0.132
Carcinogenicity	0.835	0.923	0.035	0.042
Respiratory toxicity	0.843	0.95	0.025	0.037

Protein-Ligand interaction

Selected ligands chosen as druglikeness candidates, further proceed for molecular docking analysis with standard metformin ligands. In comparative analysis, it was observed that nordiazepam showed the best affinity (-9.3 kcal/mol) towards the 1B2Y (α-amylase), followed by akuammilan-17-ol (-7.5 kcal/mol), 1,2-benzene dicarboxylic acid (-6.6 kcal/mol) and metformin (-5.3 kcal/mol). For 5NN8 (α-glucosidase), nor-diazepam exhibited the higher affinity (-8.9 kJ/mol) followed by 1,2-benzene dicarboxylic acid (-7.2 kcal/mol), akuammilan-17-ol (-7.0 kcal/mol) and metformin (-4.7 kcal/mol). The 2D interaction and 3D receptor surface interaction poses are presented in Figure. 14. When compared to all, nor-diazepam exhibited strong binding interaction with both α-amylase and α-glucosidase protein, while metformin revealed the weakest binding affinity among all. In docking observation, the analysis revealed that plant compound from *C. cuspidatus* exhibited a significant interaction with the α-amylase protein, followed by the α-glucosidase protein.

Discussion

Chamaecostus cuspidatus also known as *Costus igneus* and Spiral Flag, has been studied for its therapeutic properties. Few studies have focused on the Costaceae family and found novel compounds such as quercetin [32], insulin-like protein [33], and diosgenin [34], which have gained attention in the development of synthetic pharmaceuticals [35]. But in India, *Chamaecostus cuspidatus* is primarily grown as an unexplored ornamental plant. Early studies on *C. cuspidatus* revealed a higher content of cardiac glycosides, polyphenols, and flavonoids; these are believed to be the primary chemicals that are responsible for providing the species with anti-inflammatory and antioxidant qualities [36]. In our investigation, we noticed that the extract had a noticeably greater phenolic concentration. Expected, frequently found polyphenolic chemicals called tannin and flavonoids are utilized in medicine to treat a variety of ailments and infections [37]. Besides offering health advantages, botanical intermediate and secondary metabolism products are essential for skin-related infection healing of wounds and antioxidant activity. Since endogenous polyphenolic compounds can prevent ROS, additional research into the phytochemicals of *C. cuspidatus* is recommended.

Different functional groups, comprising phenol, aliphatic, aromatic rings, alcohol, hydroxyl, amines, and carbonyl were indicated by distinct FTIR spectrum and the presence of the hydroxyl bioactive components, aromatic rings, and fatty acid derivatives was detected by the NMR spectrum. The GCMS chromatogram disclosed that fatty acid derivatives predominated over all other components, with particular mention made of the main fatty acids found in eaves, namely 9-octadecenamide (linolenic acid), hexadecanamide (palmitic acid), and 1,2-benzene dicarboxylic acid (phthalic acid). This derivative of fatty acids could be responsible for the plant's antibacterial properties, signaling mechanism, and stress response. This plant has sixteen chemically varied metabolites, nor-diazepam, and the indole alkaloid akuammilan-17-ol, compounds that have not previously been documented. Recently, research on *Pleione maculata* discovered the existence of nor-diazepam, which had antiviral properties when linked with the SARS-CoV-2 spike protein [38]. Remarkably, nordiazepam has anti-epileptic properties and is utilized therapeutically as a psychiatric medication [39]. Moreover, this may be a significant factor in its anti-Alzheimer potential [40]. Previous studies have identified and confirmed the presence of 30

phytochemicals in *Costus lucanusianus* [41]. To the best of our understanding, this is the first report of an alkaloid compound identified as akuammilan-17-ol alkaloid compound.

This study showed a significant relationship between polyphenols, flavonoids, and tannins, emphasizing the vital importance of which antioxidant test produced outcomes that were comparable to those from *Costus igneus.* Similarly, *C. cuspidatus* had a greater capacity to scavenge free radicals; this property may be associated with the presence of hydroxyl molecules. The significance of α-amylase and α-glucosidase enzymes in this research originates from the recognition this particular plant is frequently referred to as an insulin plant and is linked to diabetes. The study expands on previous research that demonstrates a dose-dependent inhibition by the *Costus speciosus* [42] in alcohol and aqueous extracts. In further research exhibiting dose-dependent inhibition, *C. cuspidatus* was found to have an insulin-like protein, which could be the sensitizer for cells [43]. Early research studies have shown that administering quercetin regularly helps decrease blood glucose levels. This plant contains quercetin, which may be the cause of its antioxidant and antidiabetic properties [44] [45]. Although *C. cuspidatus* has previously reported the existence of coumaric acid precursor, which may be responsible for its anti-inflammatory properties, it demonstrated a rather strong inhibition of albumin. On the other hand, few studies have been done on this chemical in coumaric acid [46].

Chemically varied structural components found in plants can suppress infections, and phthalic acid constituents may play a crucial role in both antibacterial characteristics and potential for clinical study. Interestingly, *C. cuspidatus* exhibits an active zone of inhibition in very low concentrations hence it could be a treatment plant for microbial resistance. Previous studies on *Costus speciosus* have also supported the antimicrobial property, when compared to the gram-negative bacteria gram-positive bacteria show the highest percentage of inhibition because of peptidoglycan. The main intention of in vitro anticancer activity is to identify potentially toxic compounds that can disrupt cellular functions. Although there is a significant need for more research in this field because unexplored *Insulin* plant compounds and the anticancer potential of Costaceae plants have not been fully explored in vivo this field area is yet to focus. However, several studies have demonstrated the Costaceae plants exhibit cytotoxicity against cancer lines [47]. According to some research, the chemical akuammilan-17-ol has therapeutic qualities and can process within malignant cells in the sense of cell division, proliferation, and invasion [48]. In the pharmacokinetic analysis of selected phytochemicals including nordiazepam, 1,2-benzene dicarboxylic acid, and akuammilan-17-oL ligands have druglikeness activity and higher molecular binding affinity than metformin. Therefore, further animal and human clinical investigation is necessary to validate the efficacy. However, our study result explored the nor-diazepam compound in *C. cuspidatus* leaf that can increase the attention for diabetic-related Alzheimer's disease and 1,2-benzene dicarboxylic acid and akuammilan-17-ol indicates new and novel potential as a therapeutic agent for hyperglycemia.

Conclusion

In summary, the research conducted on the phytochemical composition of *Chamaecostus cuspidatus* plant leaves has identified the presence of bioactive compounds through quantitative and qualitative

analysis. In vitro activity, including antioxidant, anti-diabetic, anti-inflammatory, antibacterial, and anti-cancer activity on the HepG2 cell line, all demonstrated IC_{50} efficacy. Selected compounds revealed ADMET properties for the potential lead molecule of the methanolic extract and showed the bioavailability and toxicity range. In computational studies, enzyme inhibition activity confirmed the strong affinity and molecular interaction with protein-ligand. In addition, the nordiazepam exhibited favorable binding energy and demonstrated safe pharmacokinetic properties in ADMET studies. Also, this is the first scientific report on akuammilan-17-ol presence in the *Chamaecostus cuspidatus* leaf.

Abbreviations

ABTS - 2,2’-Azino-bis (3-ethylbenzothiazoline-6-sulfonic acid

ADMET – Absorption Distribution Metabolism Excretion Toxicity

BSA - Bovine Serum Albumin

CO_2 – Carbon dioxide

DMEM - Dulbecco’s Modified Eagle Medium

DMSO – Dimethyl sulfoxide

DNS – 3,5-Dinitrosalicyclic acid

DPPH - 2,2'-diphenyl-1-picrylhydrayl

FDA - Food and Drug Administration

FT-NMR – Fourier transform Nuclear Magnetic Resonance Spectroscopy

FTIR - Fourier Transform Infrared Spectroscopy

FRAP – Ferric Reducing Antioxidant Power

GCMS - Gas Chromatography-Mass Spectrometry

GAE - Gallic Acid Equivalent

HPLC – High-performance liquid chromatography

H_2O_2 – Hydrogen peroxide

IC_{50} – Half maximal inhibitory concentration

MHA - Muller Hinton Agar

MTT - 3-[4,5-dimethylthiazol-2-yl]-2,5 diphenyl tetrazolium bromide

M.M - Molecular Mass

NCCS - National Centre for Cell Science

NIST - National Institute of Standards and Technology

PARC - Plant Anatomy Research Centre

PNP – p-nitrophenol

Ppm – Parts per million

QE - Quercetin Equivalent

RMSD - Root Mean Square Deviation

Rpm – Revolution per minute

ROS – Reactive Oxygen Species

TAE - Tannin Acid Equivalent

Declarations

Acknowledgments

The authors sincerely acknowledge the Vellore Institute of Technology, Vellore, India for the support and laboratory facility provided for this research.

Conflict of Interests

The authors declare that there are no conflicts of interest.

Ethics approval and consent to participate

Not applicable

Consent for publication

Not applicable

Authorship contributions

Menaka Priya Balaji – Conceptualization, Methodology, Original draft preparation, Writing- Reviewing & Editing.

Devi Rajeswari V - Supervision, Project administration, Visualization, Reviewing & Editing.

Funding

No funding was provided for the research work.

Data availability

The data that has been used is confidential.

Declaration of competing interest

The authors declare that they have no known competing financial interests or personal relationships that could have appeared to influence the work reported in this paper.

ORCID

Menaka Priya Balaji – https://orcid.org/0000-0002-0494-6579

Devi Rajeswari V - https://orcid.org/0000-0002-1914-6451

References

1. Pradeepa, R. and Mohan, V. (2021) Epidemiology of type 2 diabetes in India. *Indian J. Ophthalmol.* 69, 2932–2938
2. Beros, A. *et al.* (2023) Association of arterial stiffness and neuropathy in diabetes: A systematic review and meta-analysis. *BMJ Open Diabetes Res. Care* 11, 1–12
3. Yao, D. and Brownlee, M. (2010) Hyperglycemia-induced reactive oxygen species increase expression of the receptor for advanced glycation end products (RAGE) and RAGE ligands. *Diabetes* 59, 249–255
4. Zhu, J. *et al.* (2020) The inhibitory effects of flavonoids on α-amylase and α-glucosidase. *Crit. Rev. Food Sci. Nutr.* 60, 695–708
5. Hossain, U. *et al.* (2020) An overview of the role of bioactive α-glucosidase inhibitors in ameliorating diabetic complications. *Food Chem. Toxicol.* 145, 111738
6. Stein, S.A. *et al.* (2013) A review of the efficacy and safety of oral antidiabetic drugs. *Expert Opin. Drug Saf.* 12, 153–175
7. Twaij, B.M. and Hasan, M.N. (2022) Bioactive Secondary Metabolites from Plant Sources: Types, Synthesis, and Their Therapeutic Uses. *Int. J. Plant Biol.* 13, 4–14

8. Ehikioya, C.O. *et al.* (2023) Carbohydrate digestive enzyme inhibition, hepatoprotective, antioxidant and antidiabetic benefits of Persea americana. *Sci. Rep.* 13, 1–12
9. Tchamgoue, A.D. *et al.* (2015) *Costus afer* Possesses Carbohydrate Hydrolyzing Enzymes Inhibitory Activity and Antioxidant Capacity *In Vitro*. *Evidence-Based Complement. Altern. Med.* 2015, 987984
10. Shaikh, J.R. *et al.* (2020) Qualitative tests for preliminary phytochemical screening : An overview Qualitative tests for preliminary phytochemical screening : An overview. DOI: 10.22271/chemi.2020.v8.i2i.8834
11. Kim, H.K. *et al.* (2010) NMR-based metabolomic analysis of plants. *Nat. Protoc.* 5, 536–549
12. Ramasubramaniyan, M. *et al.* (2015) Studies on Optimization of Medium in Induction and Regeneration of Callus and Shoot from Costus igneus and its Phytochemical Profile. *J. Acad. Ind. Res.* 4, 75
13. Bakshi, A. *et al.* (2022) Comparative evaluation of in vitro antioxidant and antidiabetic potential of five ethnomedicinal plant species from Punjab, India. *South African J. Bot.* 150, 478–487
14. Nikzad, N. and Parastar, H. (2021) Evaluation of the effect of organic pollutants exposure on the antioxidant activity, total phenolic and total flavonoid content of lettuce (Lactuca sativa L.) using UV–Vis spectrophotometry and chemometrics. *Microchem. J.* 170, 106632
15. Chau, T.P. *et al.* (2023) Optimization of extraction and quantification of Flavonoids from Averrhoa bilimbi fruits using RP-HPLC and its correlation between total flavonoids content against antimicrobial activity. *Appl. Nanosci.* 13, 1293–1300
16. Petchidurai, G. *et al.* (2019) Standardization and quantification of total tannins, condensed tannin and soluble phlorotannins extracted from thirty-two drifted coastal macroalgae using high-performance liquid chromatography. *Bioresour. Technol. Reports* 7, 100273
17. Shori, A.B. (2015) Screening of antidiabetic and antioxidant activities of medicinal plants. *J. Integr. Med.* 13, 297–305
18. Garcia, C. and Blesso, C.N. (2021) Antioxidant properties of anthocyanins and their mechanism of action in atherosclerosis. *Free Radic. Biol. Med.* 172, 152–166
19. Aryal, S. *et al.* (2019) Total Phenolic Content, Flavonoid Content and Antioxidant Potential of Wild Vegetables from Western Nepal. *Plants (Basel, Switzerland)* 8,
20. Dilshad, R. *et al.* (2022) Phytochemical profiling, in vitro biological activities, and in-silico molecular docking studies of Typha domingensis. *Arab. J. Chem.* 15, 104133
21. Bhuyan, B. and Chetia, D. (2019) Caracterización de compuestos antidiabéticos potentes de Costus pictus D. Don encontrados en Assam, India usando métodos in vitro e in vivo. *Ars Pharm.* 60, 15–25
22. Kim, Y.M. *et al.* (2005) Inhibitory effect of pine extract on α-glucosidase activity and postprandial hyperglycemia. *Nutrition* 21, 756–761
23. Russo, D. *et al.* (2015) Evaluation of antioxidant, antidiabetic, and anticholinesterase activities of smallanthus sonchifolius landraces and correlation with their phytochemical profiles. *Int. J. Mol. Sci.* 16, 17696–17718

24. Williams, L.A.D., *et al.* (2008) The in vitro anti-denaturation effects induced by natural products and non-steroidal compounds in heat-treated (immunogenic) bovine serum albumin is proposed as a screening assay for the detection of anti-inflammatory compounds, without the use of an animal. *West Indian Med. J.* 57, 327–331
25. Ashwin, R.S. *et al.* (2022) In vitro and silico studies on the antioxidant and anti-inflammatory potential of Piperine extracted from Piper nigrum. *Res. J. Biotechnol.* 18, 75–83
26. Williams, L.A.D., *et al.* (2008) The in vitro anti-denaturation effects induced by natural products and non-steroidal compounds in heat-treated (Immunogenic) bovine serum albumin is proposed as a screening assay for the detection of anti-inflammatory compounds, without the use of animals. *West Indian Med. J.* 57, 327–331
27. Sreena, K. and Nair, S.S. (2016) Evaluation of the anti-inflammatory activity of the plant extract Smithia Sensitiva. *Der Pharm. Lett.* 8, 310–314
28. Khalil, M.I.M., *et al.* (2015) Trigonella foenum (Fenugreek) induced apoptosis in hepatocellular carcinoma cell line, HepG2, mediated by upregulation of p53 and proliferating cell nuclear antigen. *Biomed Res. Int.* 2015,
29. Gheena, S. and Ezhilarasan, D. (2019) Syringic acid triggers reactive oxygenspecies–mediated cytotoxicity in HepG2 cells. *Hum. Exp. Toxicol.* 38, 694–702
30. Tijjani, H. *et al.* (2022) Chap. 14 - In silico insight into the interaction of 4-aminoquinolines with selected SARS-CoV-2 structural and nonstructural proteins. In *Drug Discovery Update* (Egbuna, C. B. T.-C. D. D., ed), pp. 313–333, Elsevier
31. Bender, B.J. *et al.* (2021) A practical guide to large-scale docking. *Nat. Protoc.* 16,
32. Papakyriakopoulou, P. *et al.* (2022) Potential Pharmaceutical Applications of Quercetin in Cardiovascular Diseases. *Pharmaceuticals* 15, 1–23
33. Das, K. *et al.* (2014) Extraction, estimation and comparison of proteins and carbohydrates from different parts of Costus speciosus and a brief study on its phytochemicals content. *Int. J. Basic Appl. Biol.*
34. Jesus, M. *et al.* (2016) Diosgenin: Recent Highlights on Pharmacology and Analytical Methodology. *J. Anal. Methods Chem.* 2016, 4156293
35. Yang, H. *et al.* (2016) A more ecological and efficient approach for producing diosgenin from Dioscorea zingiberensis tubers via pressurized biphase acid hydrolysis. *J. Clean. Prod.* 131, 10–19
36. Yadav, M. *et al.* (2014) Preliminary phytochemical screening of six medicinal plants used in traditional medicine. *Int. J. Pharm. Pharm. Sci.* 6, 539–542
37. Pizzi, A. (2021) Tannins medical/pharmacological and related applications: A critical review. *Sustain. Chem. Pharm.* 22, 100481
38. Sympli, H.D. (2021) *Estimation of drug-likeness properties of GC–MS separated bioactive compounds in rare medicinal Pleione maculata using molecular docking technique and SwissADME in silico tools*, 10Springer Vienna.

39. Takahashi, S. *et al.* (2021) Examination of the antiepileptic effects of valacyclovir using kindling mice— search for novel antiepileptic agents by drug repositioning using a large medical information database. *Eur. J. Pharmacol.* 902, 174099
40. Mohamed, D.A. *et al.* (2022) Ameliorative Effect of Probiotic-Fermented Milk and Costus Extract in Alzheimer's Disease Model Induced by D-Galactose and Aluminum Chloride. *Egypt. J. Chem.* 65, 411–421
41. Gherraf, N. *et al.* (2017) Chemical constituents and antimicrobial activity of essential oils of Ammodaucus leucotricus. *Arab. J. Chem.* 10, S2476–S2478
42. Pizon, J.R.. *et al.* (2018) In-vitro alpha-amylase inhibitory activity, antioxidant potential, and GCMS analysis of Crepe ginger (Costus speciosus (J. KOENIG.) SM) leaves. *Int. J. Pharm. Sci. Res.* 9, 1–23
43. Costa, I.S. *et al.* (2020) Insulin-Like Proteins in Plant Sources: A Systematic Review. *Diabetes, Metab. Syndr. Obes.* 13, 3421–3431
44. Jaishree, V. and Narsimha, S. (2020) Swertiamarin and quercetin combination ameliorates hyperglycemia, hyperlipidemia, and oxidative stress in streptozotocin-induced type 2 diabetes mellitus in Wistar rats. *Biomed. Pharmacother.* 130, 110561
45. Peasari, J. Reddy, *et al.* (2018) Chromatographic analysis of phytochemicals in Costus igneus and computational studies of flavonoids. *Informatics Med. Unlocked* 13, 34–40
46. Khan, M.F. and Ramu, A. (2018) Spectral characterization of bioactive compounds from Costus pictus and Costus speciosus. *Int. J. ChemTech Res.* 11, 353–363
47. Sathuvan, M. *et al.* (2012) In Vitro Antioxidant and Anticancer Potential of Bark of Costus pictus D.DON. *Asian Pac. J. Trop. Biomed.* 2,
48. Ramirez, A. and Garcia-Rubio, S. (2005) Current Progress in the Chemistry and Pharmacology of Akuammiline Alkaloids. *Curr. Med. Chem.* 10, 1891–1915

Figures

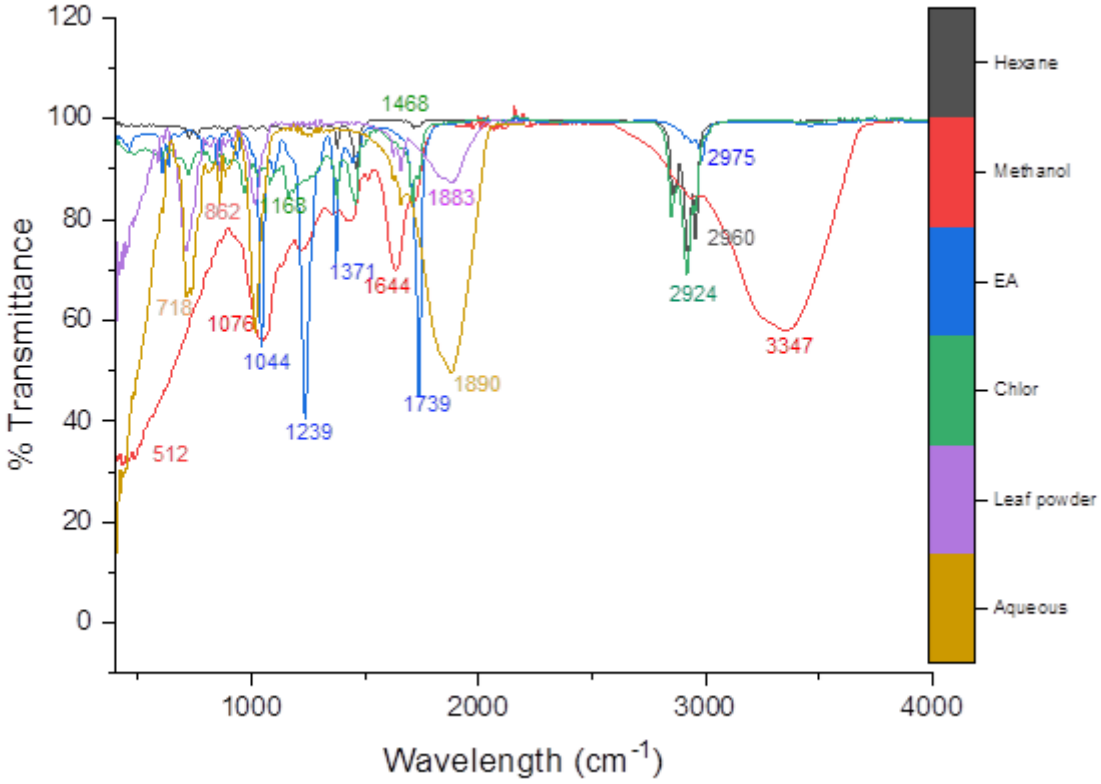

Figure 1

FTIR spectrum of *Chamaecostus cuspidatus* leaf

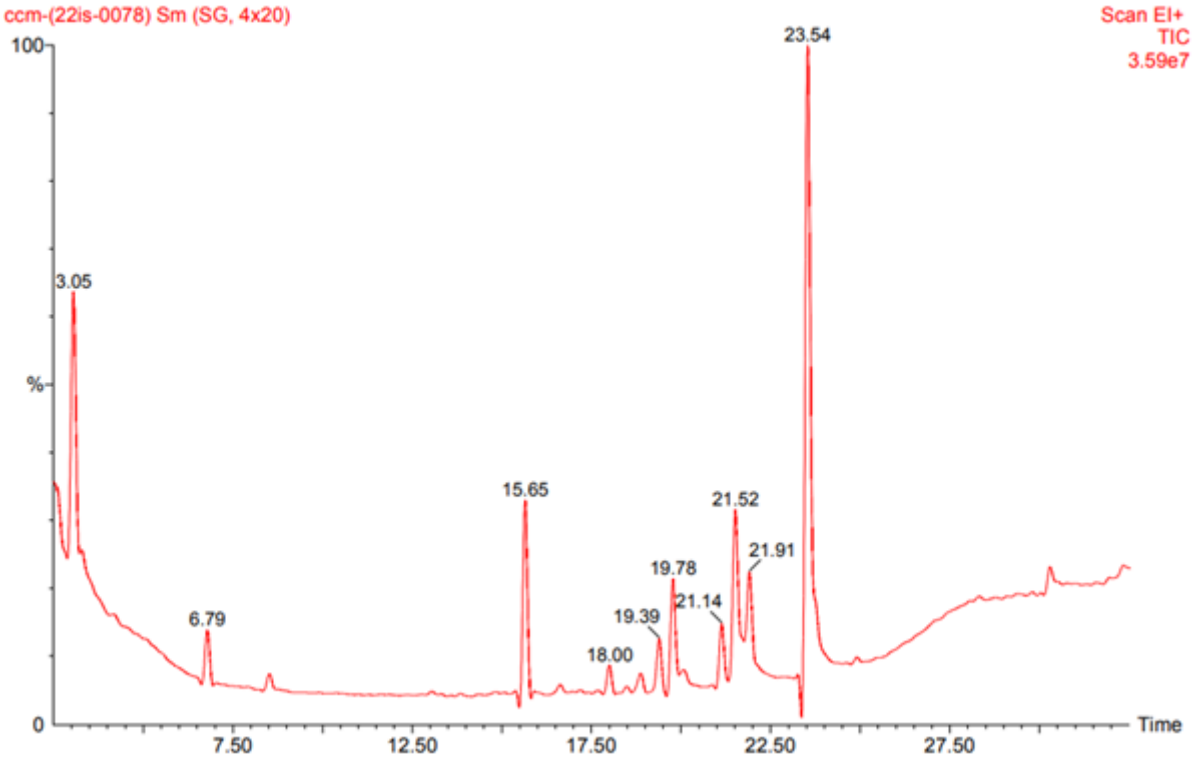

Figure 2

GC-MS analysis of *Chamaecostus cuspidatus* leaf

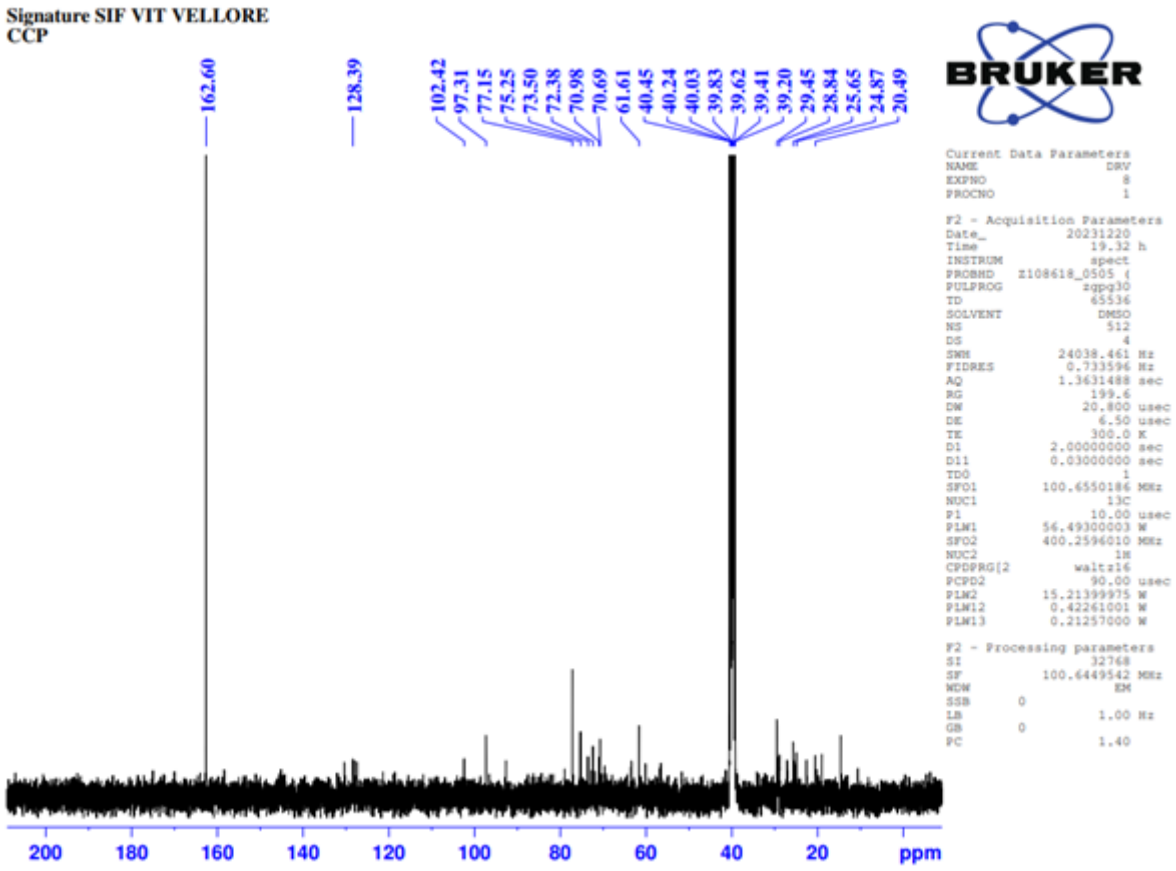

Figure 3

NMR spectrum 13C spectrum of *C. cuspidatus* leaf extract

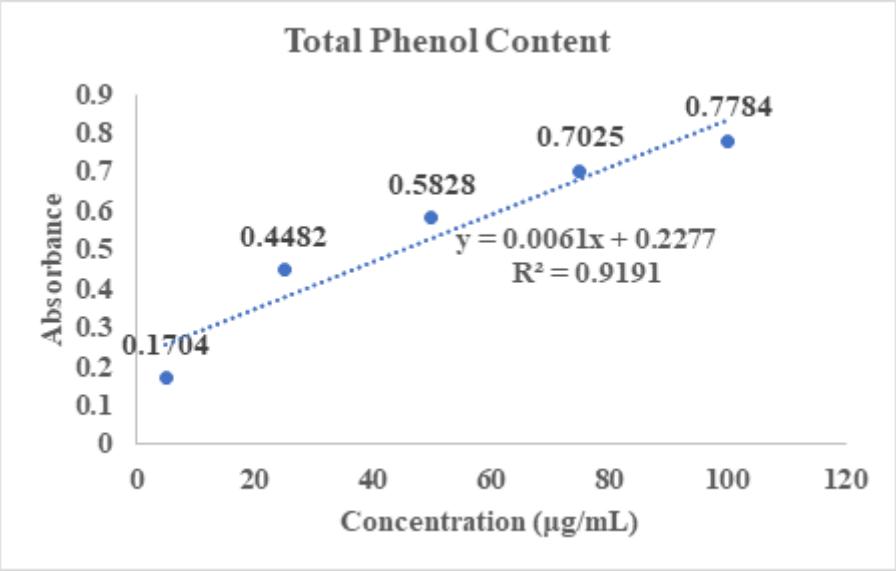

Figure 4

Gallic acid calibration curve of total phenolic content

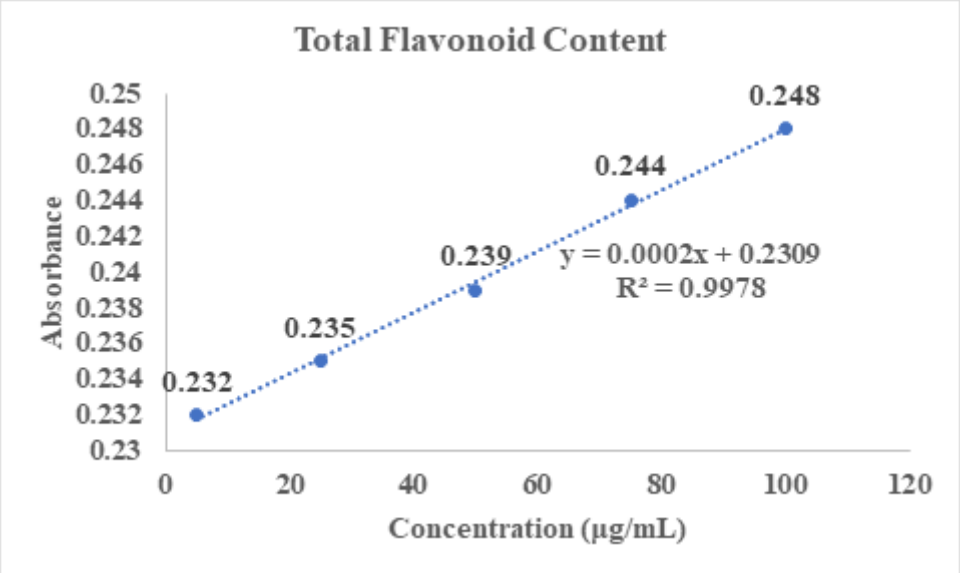

Figure 5

Quercetin calibration curve of total flavonoid content

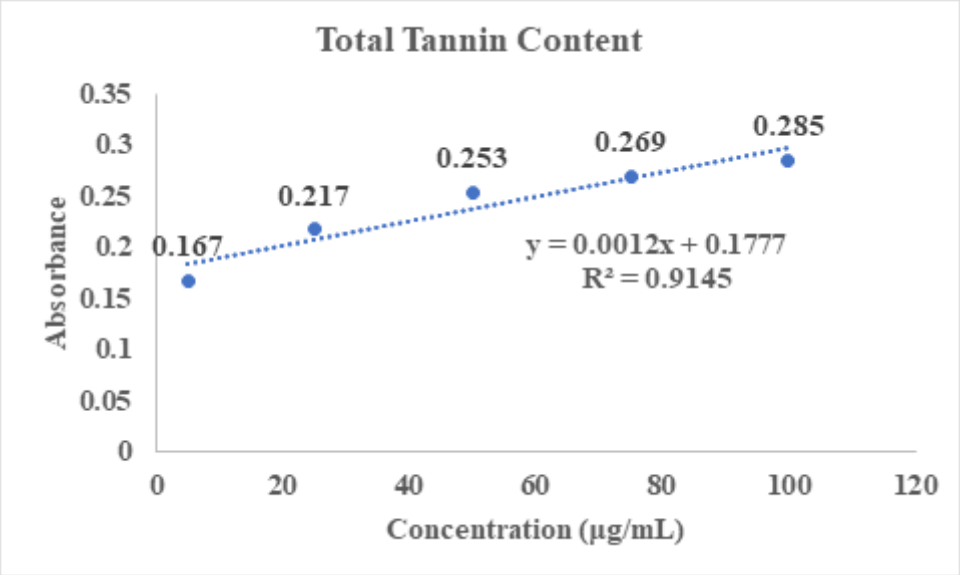

Figure 6

Tannic acid calibration curve of total tannin content

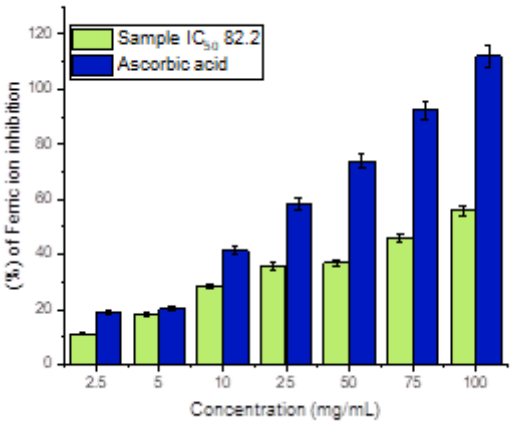

Figure 7

Comparative bar graph for FRAP assay of *Chamaecostus cuspidatus* leaf

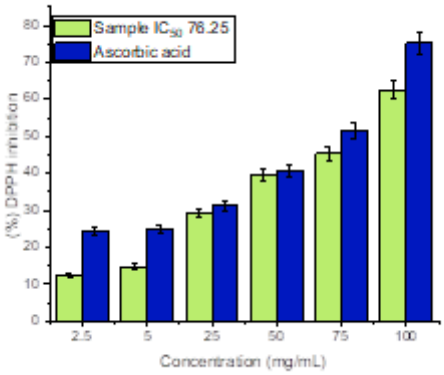

Figure 8

Comparative bar graph for DPPH assay of *Chamaecostus cuspidatus* leaf

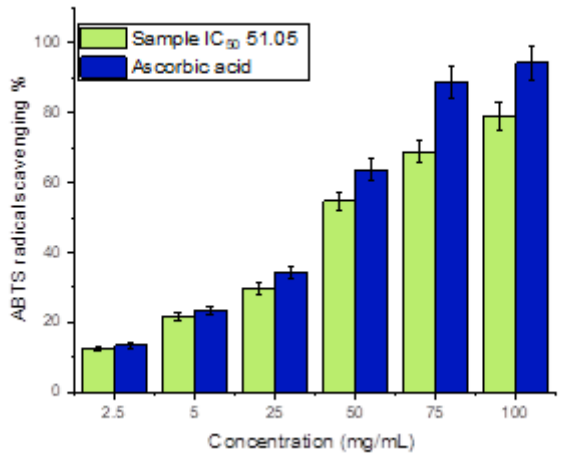

Figure 9

Comparative bar graph for ABTS assay of *Chamaecostus cuspidatus* leaf

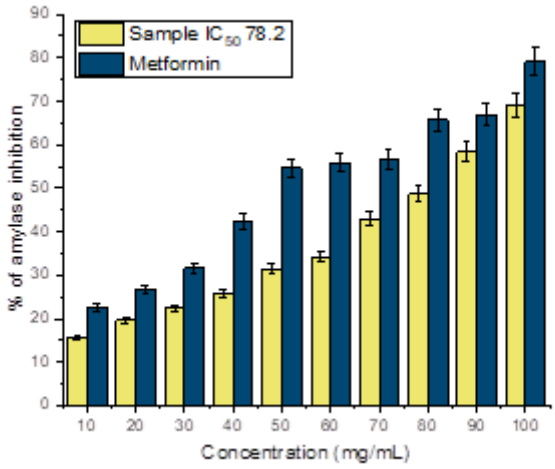

Figure 10

Comparative bar graph for α-amylase inhibitory activity of *Chamaecostus cuspidatus* leaf

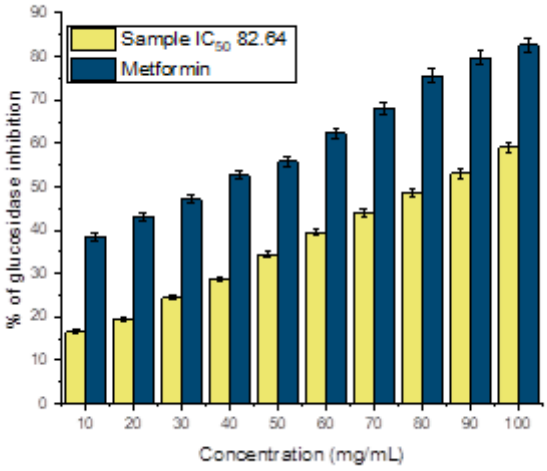

Figure 11

Comparative bar graph for α-glucosidase inhibitory activity of *Chamaecostus cuspidatus* leaf

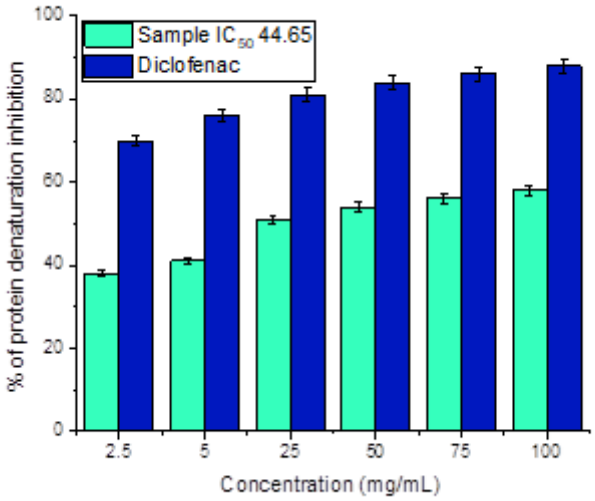

Figure 12

Comparative bar graph for protein denaturation assay of *Chamaecostus cuspidatus* leaf

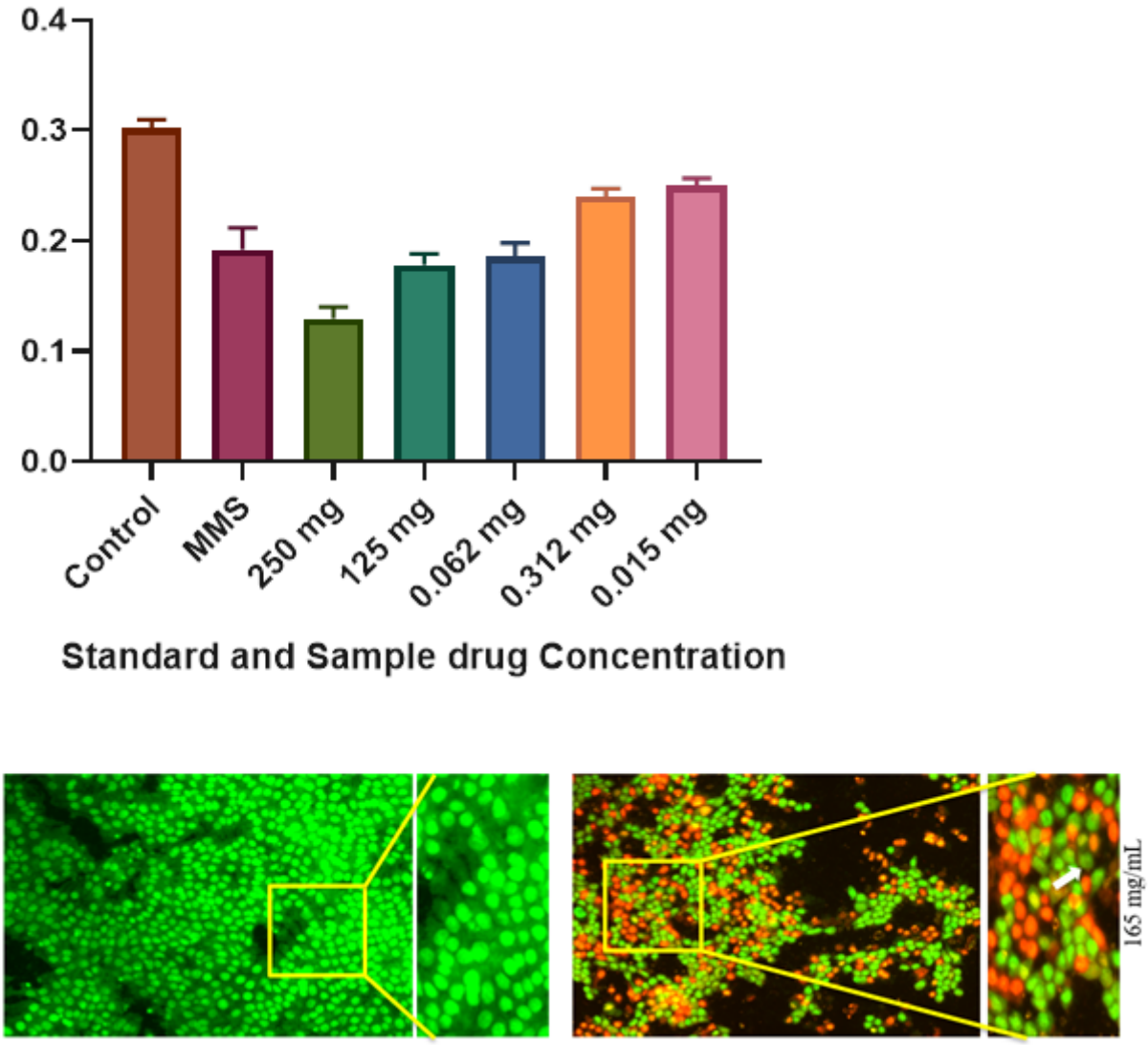

Figure 13

Comparative bar graph for HepG2 cell line and Confocal image of IC_{50} concentration

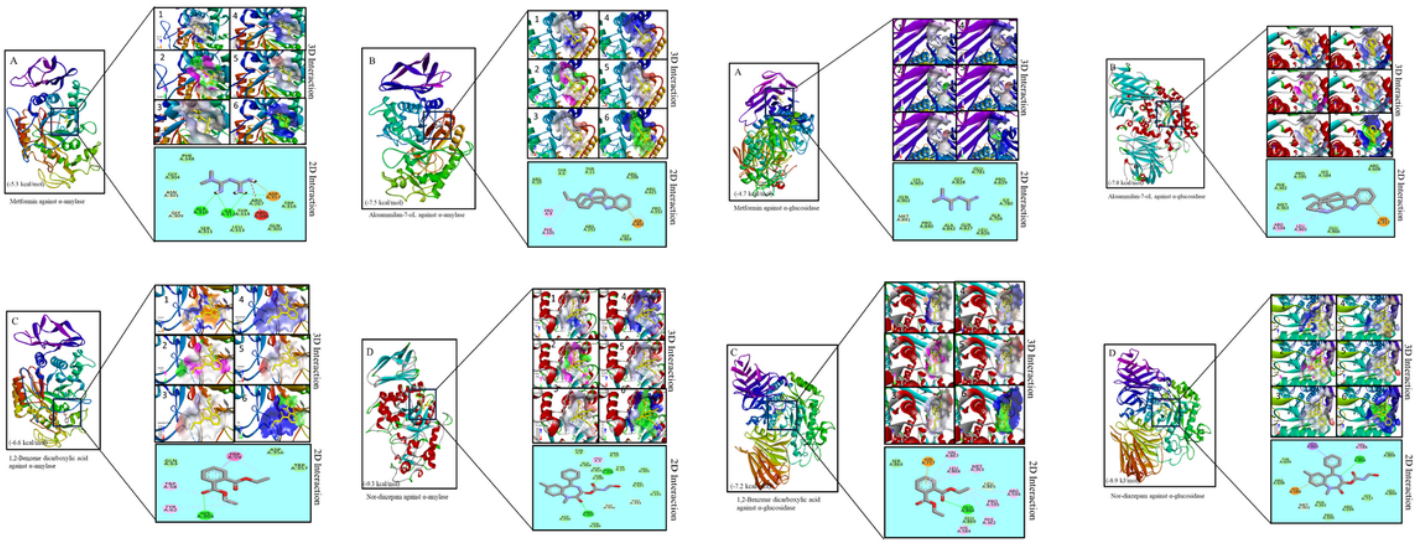

Figure 14

Molecular interaction between protein and ligand interaction

Note: 2D and 3D interactions of *C. cuspidatus* leaf phytochemicals against α-amylase and α-glucosidase proteins. A represents metformin; B represents akuammilan-17-ol; C represents 1,2-benzene dicarboxylic acid; D represents nor-diazepam. In 3D receptor surface pose 1 indicates aromatic; 2 indicates hydrogen bond; 3 indicates charge; 4 indicates hydrophobic; 5 indicates ionizability; and 6 indicates solvent accessible surface interactions between protein and ligands.

Supplementary Files

This is a list of supplementary files associated with this preprint. Click to download.

- Supplementaryfile.docx